NUMERICAL MODELLING OF EXTREME WAVE INTERACTIONS WITH A VERTICAL CYLINDER USING A PARTICLE-BASED METHOD

Taiga Kanehira, Kyoto University, taika.kanehira@gmail.com
Yuchen He, The University of Sydney, yuchen.he@sydney.edu.au
Amin Chabchoub, Kyoto University, chabchoub.amin.8w@kyoto-u.ac.jp
Nobuhito Mori, Kyoto University, mori@oceanwave.jp

INTRODUCTION

Investigation of ringing responses in marine structures is indispensable for ensuring their reliability and durability in coastal engineering. In our previous work, see He et al. (2023), we performed an experimental investigation to assess wave-induced loads on a vertical cylinder using unstable wave groups. We showed that the severe broadening of the wave spectrum triggers a ringing frequency excitation for steep wave groups. The second bound wave harmonic resonates with the lowest natural frequency of the cylinder. This does not occur when the steepnees of the carrier wave is below the steepness threshold of $(ak = 0.10)$ for the cases considered.

In this study, we aim to develop a numerical model for FSI between Peregrine-type rogue waves and a vertical cylinder following the experiments performed by He et al. (2023). The cylinder is modeled numerically as a rigid structure. This approach helps to discuss ringing response by eliminating the influence of possible resonance between the incident wave and structure in the experimental setup. Once well validated, the numerical model can provide additional insights into the ringing vibration in the laboratory experiments.

NUMERICAL MODEL AND SETTING

To simulate FSI, we use an open-source code Smoothed Particle Hydrodynamics (SPH) solver, DualSPHysics (A. Crespo et al. (2015)). The governing equations to calculate fluid motion are the Navier-Stokes equations. To reproduce the wave conditions in He et al. (2023) as closely as possible, paddle motions in our numerical simulations are generated from the same water surface elevations as in the experiments. We generate peregrine-type rouge waves with ak values of 0.07 to 0.12, where a is a wave height and k a wave frequency. Focusing waves, rogue waves, are generated by a piston-type wave maker. Due to the high computation cost, the simulation domain is constrained to the vicinity of the structure as shown in Fig. 1. The tank's length is 5 m and width 1 m. A rigid cylinder is installed in front of the paddle (x=1.25, y=0.5 m) with a constant water depth of 0.7 m. Water surface elevations and horizontal wave forces (F_x) acting on the cylinder are calculated for validation purposes of the model.

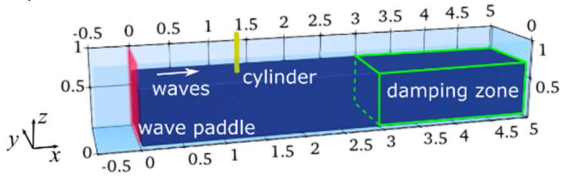

Figure 1 - Numerical wave tank used in our simulation.

Incident waves are generated by piston paddle and absorbed in the damping zone.

For numerical parameters used in this study, we use the symplectic step algorithm, Wendland kernel function, Laminar+SPS turbulence model in this study. The DDT in Fourtakas et al. (2019) is used for mDBC. The shifting method to prevent the numerical instability induced by negative pressures is not used, since the diameter of the vertical cylinder is too small (D = 55.7 mm).

NUMERICAL VALIDATIONS

In order to reduce simulation cost, we tried to derive the paddle signal from the water surface elevation, which is experimentally measured 1.25 meters in front of the cylinder's position in He et al. (2023). It is important to mention that the paddle signal derived from raw elevation data yields to fluctuations in the horizontal forces. Figure 2(d) illustrates the numerically computed horizontal forces F_x exerted on the cylinder under moderate wave steepness $(ak = 0.08)$. The forces using the paddle signal obtained from the raw elevation data are depicted by the black lines. Not that there are small fluctuations even though no ringing response is measured in the experiments (see a grey line in Fig.4(c)).

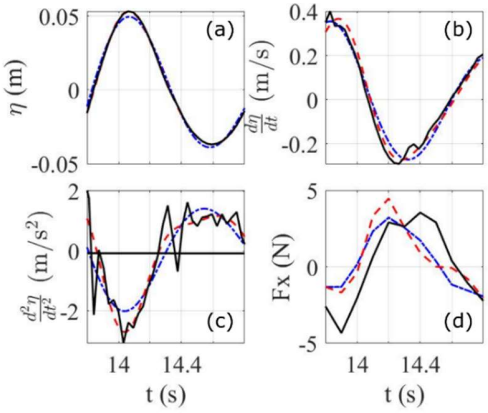

Figure 2 - Comparison of the water surface elevation $\eta(t)$ (a), first derivative of $\eta(t)$ (b), second derivative of $\eta(t)$ (c), and horizontal wave-induced forces acting on the cylinder (d). The black lines denote raw experimental data. The red line is the low-pass filtered signal with 1.5 Hz and blue 2.5 Hz.

To address this issue, first, we apply the fast Fourier transform (FFT) to the second derivative of $\eta(t)$, so that the filtered water surface elevation remains close to the

original data. Figure 2(c) shows the raw (black) and filtered (blue and red) second derivative of $\eta(t)$. The cutoff frequencies of the FFT are 1.5 Hz (blue) and 2.5 Hz (red), respectively. It is clear that high-frequency noise is effectively attenuated in Fig. 2(c), while the water surface elevation (a) and the first derivative of $\eta(t)$ (b) remain largely unchanged. Then, we calculated the paddle signal using these filtered water surface elevations and computed the horizontal wave forces acting on the cylinder in our model (as depicted in Fig. 2(d)). Clearly, fluctuations in horizontal forces are indeed significantly reduced (red and blue lines).

To validate our model, we conducted parameter study, varying three amplification factors applied to the water level $(\alpha = 0.6, 0.62, 0.66)$ to reproduce the correct boundary conditions as in the experiments, three initial particle distances ($d_p = 1.8, 1.4, 1.0$ cm), and two boundary conditions, which are implemented in the DualSPHysics (DBC and mDBC). Fig. 3 represents the distribution of the horizontal wave forces acting on the cylinder's particles under a moderate wave steepness condition $(ak = 0.08)$. It is apparent that the force distribution with the DBC Fig. 3(c) exhibits significant fluctuations compared to those using mDBC Fig. 3(d). This fluctuation is likely attributed to the presence of a gap between water free surface and the cylinder. The particle resolutions used for both DBC and mDBC were set to 1 cm. However, overall a good agreement can be seen in the case of mDBC. In mDBC, the density of solid particles is linearly extrapolated from the ghost node within the fluid domain. This method results in more accurate force calculations.

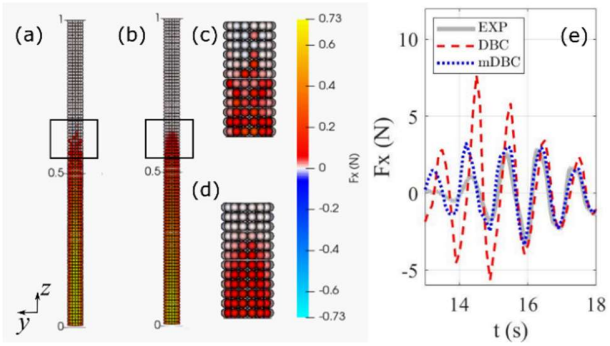

Figure 3 - Distribution of the horizontal wave forces Fx acting on the cylinder using (a,c) DBC, (b,d) mDBC. Panels (c,d) show enlarged view represented by the black square in (a,b). Panel (e) shows comparison of the wave forces F_x between experiments and SPH results (DBC or mDBC).

MAIN RESULTS

Comparisons of the water elevations and horizontal wave force acting on the cylinder are depicted in Fig. 4. Two wave conditions with a lower ak value of 0.08 and a higher value of 0.12 are shown. The comparison between SPH and laboaraotry experiments is highly consistent for the free surface. The large crest amplitude at the time of focus is compared well with the EXP in both ak values.

On the other hand, large discrepancies between measured horizontal wave faces in SPH and experiments are depicted in panels (c,d). These discrepancies would be related to the wave generation approach we used. As mentioned before, a piston-type wave maker was modeled in this study. This approach generates pressure oscillations when the non-linearity of waves gets large. We investigated the simulated pressure fields and found that significant fluctuations were observed when the largest wave was generated. It should be noted, however, that our results show good agreement except for these discrepancies, showing no ringing loads (red line) on the cylinder in panel (d) of Fig. 4. Moreover, the structure was modeled numerically as a rigid body in this study. Thus, the ringing related to resonance between the natural frequency of structure and external forces cannot be observed.

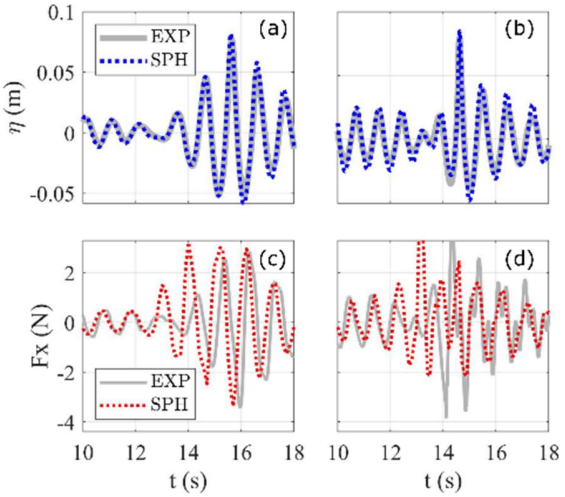

Figure 4 - Comparison of the water surface elevation $\eta(t)$ (a,b) and horizontal forces $F_x(t)$ (c,d) between SPH and EXP results. (a,c) ak value of 0.08. (b,d) ak value of 0.12.

CONCLUSIONS

We numerically simulated FSIs between a nonlinear rogue wave and a vertical cylinder using a SPH method in the 3D domain. Overall, a good agreement can be found in both moderate and severe steepness wave conditions with the limitations that no ringing responses can be observed with a rigid cylinder. FSIs using a flexible cylinder are ongoing and future studies will investigate further transient responses and the applicability of a SPH method to ocean scale problems.

REFERENCES

Y. He et al. (2023): Nonlinear and extreme wave group interactions with a circular cylinder, Proc. of the ASME 2023 42nd International Conference on OMAE.

A. Crespo et al. (2015): Dualsphysics: Open-source parallel CFD solver based on Smoothed Particle Hydrodynamics (SPH), Comput. Phys. Commun., vol.187, pp .204-216

G. Fourtakas et al. (2019): Local Uniform Stencil (LUST) boundary condition for arbitrary 3-D boundaries in parallel smoothed particle hydrodynamics (SPH) models. Computers & Fluids, Vol. 190, pp .346-361